International Journal of Pharmacy and Pharmaceutical Sciences

ISSN- 0975-1491 Vol 8, Issue 1, 2016

Original Article

STUDIES ON THE GROWTH, CHARACTERIZATION, PHYSICOCHEMICAL PROPERTIES AND ANTI-BACTERIAL ACTIVITY OF FERULIC ACID CRYSTALS

M. SANGEETHA, R. MATHAMMAL*

Department of Physics, Sri Sarada College for Women (Autonomous), Salem 636016, India
Email: mathammals_shanmugam@yahoo.com

Received: 15 Aug 2015 Revised and Accepted: 18 Nov 2015

ABSTRACT

Objective: The main objective of this research is to study the chosen Ferulic acid for pharmaceutical application through crystal growth technique. The interest of growing crystals helps in studying the physical and chemical properties of the title compound. The computational method provides a detailed interpretation of the compound under study.

Methods: Crystallization from solution is a very crucial process in the manufacture of active pharmaceutical ingredients (APIs). Ferulic acid (FA) corresponds to monohydroxylatedcinnamic acid. The biological efficiency of this kind of phenolic systems is expected to be dose-and structure-dependent, which renders the studies for the understanding of their multi-functional biological action. In the present work, ferulic acid crystals were grown using slow evaporation technique. The crystalline nature was revealed from the powder x-ray diffraction technique. The functional groups were determined using FTIR and FT-RAMAN spectra and compared with the theoretical data obtained using computational DFT method. Thermal and physicochemical stability of the grown crystal was examined by Thermogravimetric analysis (TGA) and Differential thermal analysis (DTA) studies. The charge transfer within the molecule was studied with the help of Natural Bond Orbital (NBO) analysis. The anti-bacterial activity was carried out for the title compound using disc diffusion method. The test compounds were screened *in vitro* for their antibacterial activity against two Gram-positive species (B. cereus and B. substilis) and three Gram-negative species (E. coli, P. vulgaris and S. typhi) of bacterial strains by the disc diffusion method.

Results: The grown crystal was pure and crystalline in nature. The functional groups were confirmed by FTIR and FT-Raman analysis. The melting point of the sample was found to be 172 °C. The HOMO-LUMO energy gap was calculated as 3.87eV. The first hyper polarizability was found to be 10.612 x 10-30 esu. The molecular geometry revealed the Cs symmetry of the molecule. NBO analysis confirmed the intramolecular charge transfer from lone pair oxygen atom to π*(C1-C6) and σ*(C17-O19). The compound is dominant for the B. substilis organism which is revealed from the zone of inhibition.

Conclusion: The grown Ferulic acid crystals confirmed to have good anti-bacterial activity and the theoretical study proves the biological activity of the compound.

Keywords: Ferulic acid, Crystal growth, PXRD, Anti-bacterial activity.

INTRODUCTION

Crystal growth is an eminent technique used widely for drug design. Understanding of the crystalline state leads to an understanding of the drug properties, which is crucial for many of the activities of the pharmaceutical industry. Ferulic acid is a flavonoid component with anti-oxidant property. Prior to the development of dosage forms for a new drug candidate, it is essential that certain fundamental physical and chemical properties of the drug molecule and other derived properties of the drug powder are determined [1].

The crosslinking properties of FA with both polysaccharides and proteins suggests that it can be used in the preparation of complex materials to be used in biomedical [2], pharmaceutical [3], food [4] and cosmetic applications [5]. In recent years, there have been an increasing number of reports on the physiological functions of FA and its derivatives in humans, including antioxidant, antifungal, anti-inflammatory, anti thrombosis, and anticancer activities [6-9]. Ferulic acid possesses a wide spectrum of antimicrobial activity. It exhibited antimicrobial activity towards Gram-positive bacteria, Gram-negative bacteria and yeasts [10]. The physical, chemical and the biological activity of the chosen compound is studied in detail experimentally and theoretically for future pharmaceutical applications.

MATERIALS AND METHODS

Crystal growth

Analytical grade ferulic acid and ethanol was purchased from Avra Company and used without any further purification. Ethanol was used as solvent and ferulic acid was dissolved in 30 ml of it. Single ferulic acid crystals were grown from supersaturated solution by slow solvent evaporation solution growth technique. Pale yellow coloured crystals were obtained within 2 w and it is shown in fig. 1.

Fig. 1: As grown crystals of Ferulic acid (FA)

Characterization techniques

In order to investigate the grown crystals, it was subjected to Powder X-ray diffraction, FTIR, FT-Raman spectra, TG/DTA analysis and anti-bacterial activity. The sample was prepared using a KBr

disk technique because of solid state. The FT-IR spectrum of the sample was recorded in the region 400–4000 cm-1 on a Perkin Elmer FT-IR BX spectrometer calibrated using polystyrene bands. The FT-Raman spectrum of the sample was recorded using 1064 nm line of Nd: YAG laser as excitation wave length in the region 0–4000 cm-1 on Brucker FRA 106/S FT-Raman spectrometer. The powder X-ray diffraction were studied using a Rich Seifert X-ray diffractometer employing Cu Ka (1.54058 Å) radiation, scanning angle ranging from 100 to 700 at a scan rate 10/min to confirm the crystalline phase of the grown crystal. The thermal analyses were carried out simultaneously employing NETZSCH STA409 C/CD instruments between the temperature 20 and 600 ◦C ata heating rate of 2K/m in nitrogen atmosphere.

Theoretical studies

The quantum chemical calculation of ferulic acid has been performed with the standard density functional triple-parameter hybrid model DFT/B3LYP. The 6-31+G (d,p) basis set have been employed using the Gaussian 09 program. The natural bonding orbitals (NBO) calculations [11] were performed using NBO 3.1 program in order to understand various second-order interactions between the filled orbitals of one subsystem and vacant orbitals of another subsystem, which is a measure of the intermolecular delocalization or hyper conjugation. According to the Koopman's theorem, the electronic properties of the molecules were calculated from the total energies. The important quantities such as electronegativity (χ), hardness (η), softness (S), and electrophilicity index (ψ) were deduced from ionization potential and electron affinity values.

RESULTS AND DISCUSSION

Powder X-ray Diffraction studies

The powder XRD studies were conducted to study the physicochemical characteristics of the grown crystals. XRD spectra for the crystals are presented in fig. 2. In the powder diffractogram, sharp peaks at diffraction angles (2θ) 8.870, 12.600, 15.400, 24.470, 25.610, 26.120, 29.170, 31.290, 37.760, 43.560 and 44.570 were obtained in the case of ferulic acid. The grown ferulic acid crystals belong to monoclinic system and the cell parameters are a=4.6405Ao, b=16.824Ao, c=12.019 A o, β=90.15 °, V= 938.4 (1) Ao 3. The sharp intensity peaks found in spectra shows good crystalline nature and purity of the grown crystal.

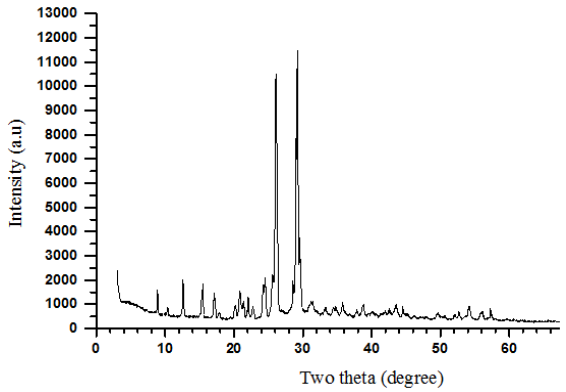

Fig. 2: Powder X-ray diffraction pattern of Ferulic acid

Molecular geometry

The geometrical parameters bond length, bond angle and dihedral angle of the chosen molecule were determined using the computational method DFT/B3LYP with the basis set 6-31+G**. The stability of the molecule was analysed by the energies obtained from the various conformers. From the conformational study, the global minimum energy was found to be-688.00953405 a. u and the optimized structure is given in fig. 3. The C1-C2, C1-C6 and C4-C5 bond length values were approximately 1.39 A0, whereas C2-C3, C3-C4 and C5-C6 were 1.41A0. This difference in the C-C bond length is due to the presence of the acid, methoxy and hydroxyl group attached to the ring carbon. The C3-C13 and C15-C17 bond length were quite increased to 1.4581 and 1.4655 A0, is due to the effect of the ethylene and the acid group attached to them. The C13-C15 has the smallest length 1.3612A0, which proves its double bond character. The C-O bonds take the same value approximately, whereas C=O bond is reduced depicting the double bond nature.

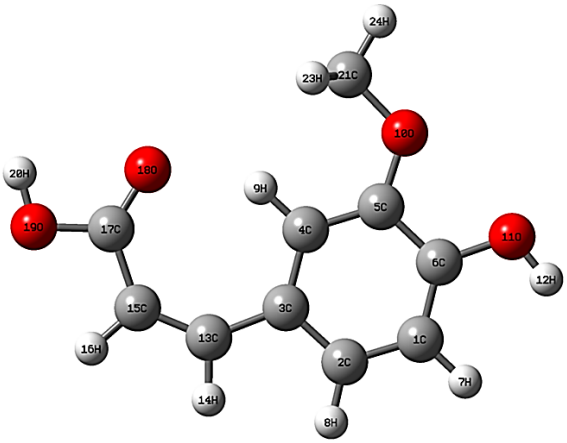

Fig. 3: Optimized structure of Ferulic acid

The C–H bond values lies in the same range except for the bond nearby the methoxy group. The effect of electronegative oxygen atom has increased the bond length slightly. The distortion in the hexagonal symmetry of the ring has been proved from the variation in the bond angles.

Natural bond orbital (NBO) analysis

NBO analysis is an important tool for studying hybridization, covalence effects, hydrogen bonding and Van der Waals interactions [12]. A useful aspect of the NBO method is that it gives information about interactions of both filled and virtual orbital spaces that could enhance the analysis of intra and inter molecular interactions. The intra-molecular hyper-conjugative interactions are formed by the orbital overlap between π* C1-C6 and π * (C4–C5) bond orbitals which results in ICT causing stabilization of the system. The strong intra-molecular hyper conjugative interaction of C4–C5 from π* C1-C6 →π* C4 -C5* which increases ED (0.34111e) that weakens the respective bonds leading to stabilization of 214.09 kcal mol-1.

The interaction π(C13-C15) → π *(C17 –O18) are responsible for conjugation of respective π-bonds due to the high electron density at π bonds (1.84930), low density at π* bonds (0.29278) and stabilized the molecule with energy in the region 23.08 kcal/mol. The interactions π (C1-C6) →π*(C2 -C3), π (C2-C3) →π*(C4 -C5), π (C4-C5) →π*(C2 -C3) demonstrate strong π–electron delocalization within the ring stabilized the molecule with E(2) max~ 19.28 kcal/mol. The interactions between n2 (O11) →π*(C1 -C6), n2 (O18) →σ*(C17-O19) leads to an enormous stabilization of 29.40 kcal/mol and 33.67 kcal/mol. This strong stabilization denotes the larger delocalization. This highest interaction around the ring can induce the large bioactivity in the compound.

Frontier molecular orbitals

To explain several types of reactions and for predicting the most reactive position in conjugated systems, molecular orbitals and their properties such as energy are used [13]. The most important orbitals in the molecule are Highest Occupied Molecular Orbital (HOMO) and Lowest Unoccupied Molecular Orbital (LUMO). The energy gap between the HOMO and LUMO reflect the biological activity of the molecule. In the present compound, the HOMO is localized all over the C-C in the phenyl ring and COOH group and LUMO is localized

over the CH_3 group. This shows a significant electron density transfer among the ring and its substituent's. In order to study the various aspects in pharmacology and characteristics of the drug molecule, new chemical reactivity descriptors have been proposed. DFT based descriptors have helped in many ways to understand the structure of molecules and their reactivity by calculating the chemical potential, global hardness and electrophilicity. The calculations show that the title compound has 51 occupied orbitals and the HOMO and LUMO energies are-5.9439eV and-2.0730eV respectively.

Using HOMO and LUMO energy values for a molecule, electronegativity, chemical hardness and chemical softness can be calculated as follows:

$$\chi = I+A/2 \text{ (Electronegativity)},$$

$$\eta = I-A/2 \text{(Chemical hardness)},$$

$$S = 1/2\eta \text{ (Chemical softness)},$$

where Iand A are ionization potential and electron affinity;

$$I = -E_{HOMO}$$

$$A = -E_{LUMO}$$

Respectively [14]. The HOMO and LUMO energies, the ionization potential (I), the electron affinity (A), the absolute electronegativity (χ), the absolute hardness (η) and softness(S) for molecule have been calculated at the same levels and the results are 5.9439eV, 2.0730eV, 4.0085eV, 1.9355eV and 0.2583eV respectively.

NLO properties

NLO studies are a key technique for the emerging technologies in the field of telecommunications, signal processing and optical instrumentations. Theoretical calculation on the parameters such as polarizabilities and hyper-polarizabiities are quite useful in understanding the structural relationship between the molecule and its non-linear optical property. The γ_{orient} was calculated using the relation,

$$\gamma_{orient} = D\Delta\alpha^2$$

Where D is a constant depending on Boltzmann constant (k) and temperature (T). If Δα is in a. u., the constant D=7.902868 $x10^{-3}$ then γ_{orient} is in 10^{-36} esu. The first-order hyper polarizability (β), the orientational second-hyper polarizability (γ_{orient}) and related properties (μ, α and Δα) are calculated for the title compound using B3LYP/6-31+G** method and gathered in table 1.

The tabulated NLO parameters are compared with a prototypical molecule with the similar properties. Here, p-nitroniline (p-NA) is chosen for reference [15] and the calculated values are compared with it. The first hyper polarizability value for the title compound is 10.612 x 10^{-30} esu, whereas for p-NA it is 11.54 x 10^{-30}esu. From these values, it clearly proves that the molecule has good NLO property and used for non-linear applications.

Table 1: Total dipole moment (μ, in Debye), the mean polarizability (α, in 10^{-24} esu), the anisotropy of the polarizability (Δα, in 10^{-24} esu), the mean first-order hyper polarizability (β, in 10^{-30} esu) and the orientational second-order hyper polarizability (γ_{orient}, in 10^{-36} esu) for Ferulic acid

Dipole moment		Polarizability		First and second hyper polarizability	
		α_{xx}	222.755	β_{xxx}	-2000.024
μ_x	0.1627	α_{xy}	-16.763	β_{xxy}	155.451
μ_y	-0.7308	α_{yy}	153.169	β_{xyy}	-188.875
μ_z	0.1113	α_{xz}	3.361	β_{yyy}	-177.257
μ	0.7569	α_{yz}	-11.965	β_{xxz}	-33.703
		α_{zz}	76.632	β_{xyz}	18.391
		α	22.36	β_{yyz}	4.512
		Δα	131.66	β_{xzz}	-78.892
				β_{yzz}	-69.123
				β_{zzz}	30.472
				β_0	10.612
				γ_{orient}	3008.77

Thermal analysis

Thermogravimetric (TG) and differential thermal analysis (DTA) were carried out using a Perkin Elmer STA 6000 thermal analyser in nitrogen atmosphere. The sharp endothermic peak at 172 ° C indicates the melting point of the compound. The crystallinity and the purity of the crystal are clearly understood from the sharpness of the peak. The TG curve shows a single stage weight loss at ~ 210 ~ 420 ° C and it is due to the decomposition of ferulic acid into fragments and their subsequent volatilization.

Vibrational analysis

The title compound consists of 24 atoms and it belongs to C_s point group symmetry. The 66 normal modes are distributed among the symmetry species as,

$\Gamma_{3N-6} = 45A'$ (in-plane)+21A″ (out-of-plane)

And in agreement with C_s symmetry. The fundamental vibrations are calculated using DFT/B3LYP/6-31+G** method. The experimental and calculated frequencies, IR intensity, Raman activity and Potential energy distribution (PED) assignments are gathered in table 2.

Aromatic C-H vibrations

The C–H stretching vibrations of the phenyl ring are normally observed in the region 3100–3000 cm^{-1} [16-17] which shows their uniqueness of the skeletal vibrations. For the present molecule, the calculated frequencies at 3017, 3030, 3059, 3053 and 3111 cm^{-1} are assigned for C-H vibrations and the experimental IR peaks are observed at 3080 and 3017 cm^{-1}. The aromatic C-H vibrations are in the expected region and not affected by the substitution groups. The vibrations at 1278, 1232 in IR and 1275 cm^{-1} in Raman is allotted for in-plane bending vibrations. Raman peaks at 920, 886and 783 cm^{-1} are assigned for out-of-plane bending and no peaks were observed in IR. The calculated frequencies for in-plane and out-of-plane CH bending are within the region and most of the values coincide with the experimental data.

Methoxy group vibrations

The two bands observed at 2969 and 2906 cm^{-1} in IR are assigned for CH_3 stretching vibrations and the calculated values allotted for the stretching vibrations are 3003, 2962 and 2897 cm^{-1}. The calculated frequencies at 1442, 1426 and 1400 cm^{-1} are assigned for in-plane bending of CH_3 group and its corresponding experimental values obtained as 1433 cm^{-1} in IR and 1435 cm^{-1} in Raman. The CH_3 rocking vibration at 1114 cm^{-1} in IR well coincides with the theoretical value at 1119 cm^{-1} with 92% contribution. The out-of-plane bending vibrations at 250, 181 and 100 cm^{-1}also show major contribution theoretically and no experimental peaks were obtained both in IR and Raman.

Acid group vibrations

The high intensity peak at 3080 cm^{-1} in IR is assigned to the O-H stretching vibrations and the corresponding calculated peak is

obtained with 100% PED contribution. Generally a strong absorption is absorbed in 1700 cm^{-1} for C=O group indicating the presence of ketone, aldehyde, carboxylic acid or amide. Considerably the C=O stretching vibrations of acids are more intense than ketonic C=O stretching vibrations. The peak observed at 1692 cm^{-1} is allotted for C=O stretching vibration, and the calculated frequency takes the value 1685 cm^{-1}, well matching with each other.

Table 2: Vibrational analysis

Symmetry species	Observed frequencies (in cm^{-1})		Calculated frequencies (in cm^{-1})		IR intensity	Raman intensity	PED (%)
	FTIR	FT-Raman	Unscaled frequencies	Scaled frequencies			
A″		31	39	37	0.0298	0.8481	τring(54), τacid(32)
A″		41	51	49	2.0258	0.5045	τacid(90)
A″		99	101	97	6.6879	1.0491	τCH_3(89)
A′			105	100	1.3655	2.0424	βCH_3(97)
A″		112	125	120	1.3682	0.1277	τring(64), τC=C(31), τOH(10)
A″			189	181	0.0002	1.1871	τCH_3(63), τring(24)
A′			198	189	2.0241	3.3409	βCCC(58), βCH_3(23)
A′		220	251	240	5.8699	0.8806	βCH_3(87), βOH(10)
A′			261	250	0.3217	0.0721	βCCO(52), βring(11)
A′			309	295	2.6926	2.9196	βOH(51), βacid(30), τC=C(11)
A″		300	317	303	3.8274	0.4521	δCH_3(62),δOH(24),τacid(10)
A′			363	347	1.3928	8.2429	βCOC(62), βCOH(34)
A″			372	356	90.0985	1.4588	δOH(79)
A″		401	428	409	18.9239	5.2001	δC=C(59), δOH(21)
A″			471	450	2.1851	0.5314	τring(72), δOH(18)
A′			485	464	30.1050	3.1359	βCCO(68), βCCC(25)
A′			533	510	7.3035	2.0769	βCOC(64), βOH(13), βOH_{acid}(11)
A′			550	526	15.7777	5.2824	βCH_3(51), βOH(23), βring(11)
A″			576	551	71.8209	0.9211	δOH (67),δring (14)
A′			596	570	36.3559	5.0193	βCOH (69), βOH(13)
A″	581		616	589	27.9466	4.0593	δring (52), δOH(23)
A″		672	715	684	2.6619	12.8378	δring(67), δOH(24),δCH(10)
A′	690		719	687	11.3740	1.4017	βCCC(79), βOH(11)
A″			748	715	13.0235	0.1578	δring (91)
A′		720	763	729	5.6540	16.4018	βCCC(71), βring(29)
A″		783	809	773	7.8842	0.6181	δCH(86)
A′	750		812	776	22.4371	23.5323	βring(82), βOH(17)
A″	805	810	841	804	66.6425	0.4613	δOH(83)
A′	863		902	862	18.1362	8.4910	βring(56), βOH(15)
A″		886	923	882	3.7106	0.2123	δCH(90)
A″		920	942	901	21.7903	0.1807	δCH(89)
A′	948		989	945	11.4977	2.6747	βring(42), βOH(26), νCO(10)
A″	973		1019	974	0.1707	4.9241	δCH(94)
A′	1036		1061	1014	31.6072	8.5602	νCO(80), βring(19)
A′			1143	1093	855.2172	103.8244	νCO(66), βOH(32)
A′			1147	1097	199.3150	13.9621	νCC(58),βOH(34),νCO(14)
A″	1114		1170	1119	0.9735	1.2383	CH_3rock(92)
A′			1179	1127	1.4259	4.4255	βCCO(69),βCH(45),νCC(20)
A′	1155		1200	1147	37.0149	36.0809	βCH(53), βOH(36), βCH_3(11)
A′	1178		1217	1163	2.6218	4.2673	βOH(74), βCH_3(17)
A′	1232		1285	1228	105.2868	39.6050	βCH(56),νCO(13)
A′		1246	1297	1240	2.8652	33.5247	νCO(62), βCH(19)
A′	1243		1312	1254	164.4599	9.2552	βCH(67), βOH(24)
A′	1278	1275	1331	1272	139.3413	120.3627	βCH(45),βring(25),νOH(12)
A′	1291		1353	1293	128.3795	99.2980	νCC(54),βCH(37),βOH(10)
A′	1380		1403	1341	17.5734	18.8544	νCO(65),βOH(21),βCH(10)
A′	1413		1464	1400	40.7466	64.3186	βCH_3(79), βring(14)
A′			1486	1421	30.3069	5.4840	βOH(55), βCH_3(13)
A′			1492	1426	2.1198	50.2330	βCH_3(90),βCH(42)
A″	1433	1435	1499	1433	9.3777	12.0037	δCH_3(92)
A′			1508	1442	51.9260	5.4479	βCH_3(89)
A′	1467		1555	1487	290.0398	36.5946	νCC(56),βCH(22)
A′	1518		1622	1551	316.9962	802.4046	νCC(62),βCH(31)
A′			1635	1563	150.5713	622.7839	νCC(84),βCH(12)
A′	1592		1663	1590	101.6117	282.0113	νCC(78),βCH(22)
A′	1692		1763	1685	208.3330	60.4077	νCO(67), βOH(21),βCH(10)
A′	2906		3030	2897	39.1114	118.2379	νCH_3(98)
A″	2969		3098	2962	29.1448	32.4440	νCH_3(98)
A′			3141	3003	10.7251	44.3331	νCH_3(99)
A′	3017		3156	3017	22.6296	132.6742	νCH(99)

A′		3169	3030	18.9579	129.3551	νCH(98)
A′		3194	3053	11.1349	128.1314	νCH(100)
A′		3200	3059	5.2061	158.2137	νCH(98)
A′		3254	3111	49.7387	44.2831	νCH(97)
A′	3080	3768	3602	105.8985	140.4857	νOH(100)
A′	3438	3822	3654	101.6266	274.5453	νOH(100)

ν–Stretching; β–in-plane vibrations; δ–out-of-plane vibrations; τ-torsion

C-C vibrations

Generally, the C-C stretching vibrations in aromatic compounds from six bands in the region 1650–1430 cm^{-1}. For the chosen compound, the calculated frequencies at 1590, 1563, 1551 and 1487 cm^{-1} are active in IR at 1592 and 1518 cm^{-1}. The substitution of the functional groups has shifted the band to lower wave number 1291 and 1147 cm^{-1}. The theoretical value well matches with the observed one.

The in-plane bending of the ring calculated at 945, 776 and 729 cm^{-1} has the respective experimental value at 948, 863,750 cm^{-1} in IR and 720 cm^{-1} in Raman. The out-of–plane bending vibrations at 715, 684 and 589 cm^{-1} are found to be in correlation with the observed values.

O-H vibrations

The O-H stretching vibration is assigned to the peak at 3438 cm^{-1} experimentally, whereas the theoretical frequency shows 100% PED contribution for the phenol O-H group. For the title molecule, a very weak band appears at 1178 cm^{-1} for O-H in-plane bending vibrations and the calculated data well matches with it. The calculated O-H out-of-plane bending has the value as 356 cm^{-1} with 79% PED contribution.

Anti-bacterial studies

Owing to various applications of FA in the field of medicine, it has been chosen for study. FA was reported for antibacterial activity [10] which is the extraction of FA from plant extracts and confirming its application against gram-negative and gram-positive bacteria. The present study aims in growing FA crystals for analyzing the physicochemical properties and its pharmaceutical applications. The antibacterial results were shown in table 3. The results were compared with standard control chloramphenicol.

The effect of the organisms at the concentrations 30 and 40 µg/ml was not much effective. As the concentration was increased, the chosen compound shows an effective inhibition of the microorganisms. Especially, FA was very dominant against the gram-positive bacteria (B. substilis). The zone of inhibition for B. substilis is around 19,25and 32 mm at the concentration 40, 50 and 60 µg/ml, whereas for the control the zone of inhibition is at 17 mm. Since the zone of inhibition for the chosen compound was almost greater than the control at 60 µg/ml, the triplicate value was found at that concentration and the Standard deviation is calculated. Table 4 depicts the activity of FA at the concentration 60 µg/ml for triplicate value. From the table 4, it is clear the chosen compound is very active against all the organisms.

Table 3: Antibacterial activity of Ferulic acid at different concentrations

S. No.	Organism Name	Control zone of inhibition (mm)			mean±SD	Concentration in µg/ml			
						30	40	50	60
						zone of inhibition(mm)			
1.	*E. Coli*	17	16	20	17.66±1.47	-	13	18	23
2.	*P. Vulgaris*	20	21	15	18.66±2.07	13	16	21	25
3.	*S. typhi*	19	23	18	20.0±1.87	-	12	16	24
4.	*B. Cereus*	20	25	22	22.33±1.77	12	14	17	24
5.	*B. Substilis*	17	17	18	17.33±0.40	14	19	25	32

Inhibition zone (in mm) includes the diameter of disc (6 mm); Standards: Chloramphenicol (1.0 mg/disc), Values are mean of triplicate readings (mean±SD).

Table 4: Triplicate value for FA at the concentration 60 µg/ml

S. No.	Organism	Control zone of inhibition(mm)			mean±S. D	Triplicate value			mean±S. D
1	*P. Vulgaris*	19	21	15	17.66±1.47	24	28	18	23.33±3.55
2	*S. typhi*	19	23	18	18.66±2.07	26	28	27	27±0.70
3	*B. substilis*	17	17	18	20.0±1.87	24	32	31	29±3.08
4	*B. cereus*	20	25	22	22.33±1.77	28	31	29	29.33±1.08
5	*E. coli*	17	16	20	17.33±0.40	32	34	34	33.33±0.81

Inhibition zone (in mm) includes the diameter of disc (6 mm); Standards: Chloramphenicol (1.0 mg/disc), Values are mean of triplicate readings (mean±SD).

CONCLUSION

The cell parameters of the chosen compound were determined using the Powder XRD results and found the substance to be crystalline in nature. The intramolecular interaction within the molecule and the stabilization energies were determined using NBO 3.1 program. The determination of the Frontier Molecular Orbitals (FMO) helped in understanding the characteristics of the drug molecule and the chemical activity of the compound.

The calculated electrostatic potential confirmed the solid-state interactions. The predicted hyper polarizability value of the title compound confirmed it to be a good non-linear optical material. The decomposition state of the compound was determined with the help of TG/DTA analysis and the melting point of the sample was also determined. The presence of the functional groups was studied using the FTIR and FT-Raman technique and compared with theoretical data.

Furthermore, the compound was found to have potential antibacterial activity against microbial strains.

CONFLICTS OF INTERESTS

All authors have none to declare

REFERENCES

1. Young Taek Sohn, Jin Hee Oh. Characterization of physicochemical properties of Ferulic acid. Arch Pharm Res 2003;26:1002-8.

2. Wargovich M, J Jimenez A, Mc Kee K, Steele VE, Velasco M, Woods J, Price R, *et al*. Efficacy of potential chemopreventive agents on rat colon aberrant crypt formation and progression G. J Carcinogenesis 2000;21:1149-55.
3. Mori H, Kawabata K, Yoshimi N, Tanaka T, Murakami T, Okada T, *et al*. Chemopreventive effects of ferulic acid on oral and rice germ on large bowel carcinogenesis. Anticancer Res 1999;19:3775-8.
4. Aruoma OI. Nutrition and health aspects of free radicals and antioxidants. Food Chem Toxicol 1994;32:671-83.
5. Ou S, Kwok KC. Ferulic acid: pharmaceutical functions, preparation, and applications in foods. J Sci Food Agric 2004;84:1261-9.
6. Kayahara H, Miao Z, Fujiwara. Synthesis and biological activities of ferulic acid derivatives G. Anticancer Res 1999;19:3763-8.
7. Akihisa T, Yasukawa K, Yamaura M, Ukiya M, Kimura Y, Shimizu N, Arai K. Triterpene alcohol and sterol ferulates from rice bran and their anti-inflammatory effects. J Agric Food Chem 2000;48:2313-9.
8. Xu LN, Xu DC, Zhang Z. Investigation on the mechanism of sodium ferulate in lowering blood platelet aggregation: effect of sodium ferulate on the equilibrium of TXA 2 and PGI 2. Acta Pharm Sin B 1984;6:414-7.
9. Panizzi L, Catalano S, Miarelli C, Cioni PL, Campeol. *In vitro* antimicrobial activity of extracts and isolated constituents of geumrivale E. Phytother Res 2000;14:561-63.
10. Jeong. YC, Jae HM, Keun HP. Isolation and identification of 3-methoxy-4-hydroxybenzoic acid and 3-methoxy-4-hydroxy-cinnamic acid from hot water extracts of Hoveniadulcis Thunb and confirmation of their antioxidative and antimicrobial activity. Korean J Food Sci Technol 2000;32:1403–8.
11. Glendening ED, Reed AE, Carpenter JE, Weinhold F. NBOVersion3.1 TCI, University of Wisconsin, Madison; 1998.
12. Weinhold F, Landis CR. Valency and bonding: a natural bond orbital donor–acceptor perspective. Cambridge University Press: Cambridge, New York, Melbourne; 2005. p. 215–74.
13. Choudhary N, Bee S, Gupta A, Tandon P. Comparative vibrational spectroscopic studies, HOMO–LUMO and NBO analysis of N-(phenyl)-2,2-dichloroacetamide, N-(2-chloro phenyl)-2,2 dichloroacetamide and N-(4-chloro phenyl)-2,2-dichloroacetamidebased on density functional theory. Comput Theor Chem 2013;1016:8–21.
14. Pearson RG. "Absolute electronegativity and hardness correlated with molecular orbital theory. Proc Natl Acad Sci USA 1986;83:8440–1.
15. Jug K, Chiodo S, Calaminici P, Avramopoulos A, Papadopoulos MG. Electronic and vibrational polarizabilities and hyperpolarizabilities of azoles: a comparative study of the structure-polarization relationship. J Phys Chem A 2003;107:4172-83.